Imperfections in a two-dimensional hierarchical structure

Daniel Rayneau-Kirkhope,[1] Yong Mao,[2] and Robert Farr[3,4]
[1]*Aalto Science Institute, School of Science, Aalto University, 02150 Espoo, Finland*
[2]*School of Physics and Astronomy, University of Nottingham, Nottingham NG7 2RD, United Kingdom*
[3]*Unilever R&D, Colworth House, Sharnbrook, Bedford MK44 1LQ, United Kingdom*
[4]*London Institute for Mathematical Sciences, 35a South Street, Mayfair, London, United Kingdom*
(Received 24 October 2013; published 12 February 2014)

Hierarchical and fractal designs have been shown to yield high mechanical efficiency under a variety of loading conditions. Here a fractal frame is optimized for compressive loading in a two-dimensional space. We obtain the dependence of volume required for stability against loading for which the structure is optimized and a set of scaling relationships is found. We evaluate the dependence of the Hausdorff dimension of the optimal structure on the applied loading and establish the limit to which it tends under gentle loading. We then investigate the effect of a single imperfection in the structure through both analytical and simulational techniques. We find that a single asymmetric perturbation of beam thickness, increasing or decreasing the failure load of the individual beam, causes the same decrease in overall stability of the structure. A scaling relationship between imperfection magnitude and decrease in failure loading is obtained. We calculate theoretically the limit to which the single perturbation can effect the overall stability of higher generation frames.

DOI: 10.1103/PhysRevE.89.023201 PACS number(s): 46.70.De, 46.32.+x, 46.25.Cc

Hierarchical designs are found throughout nature where optimization for one or more mechanical functions can be observed. The direction-dependent adhesive interface on the gecko's toes [1], the trabecular bone, which exhibits remarkable strength and stiffness [2,3], and spider capture silk's exceptional elasticity [4,5] are all dependent on hierarchical geometries with features over a wide range of length scales.

Recent theoretical works assessed the benefits that can be obtained from self-similar hierarchical designs [6–10]. However, in attempting to create structures of high efficiency, inevitable initial imperfections can result in problems of reliability [11]. The technique of naive optimization (used in Refs. [6–10]) is a useful tool in creating theoretical bounds for efficiency of structures. It is often the case, however, that through its implementation, high imperfection sensitivity is introduced [11]. The deviation of parameters describing a structure from their theoretical ideal is inevitable. It is therefore essential that the imperfection sensitivity is investigated before designs exploiting hierarchy can become practical [12,13].

We first introduce a two-dimensional hierarchical design and optimize it for mechanical efficiency under gentle compressive loading. We present a scaling of material required for stability against the compressive load it is required to withstand. This scaling law can be manipulated through changing the hierarchical order of the structure. We obtain the fractal dimension of the optimal structure and show a nontrivial dependence on the loading for which the structure is optimized. Then we introduce a single imperfection in the composite structure: a single central beam is perturbed. We find theoretically the effect of this perturbation on generation-1 and -2 structures. Observations on the limit of sensitivity for higher-order structures are made. The generation-1 frames are then investigated through finite-element simulations; good agreement between analytic and computational results is found.

The two-dimensional geometries that are investigated here can be thought of as cross sections of a three-dimensional structure that is assumed to be uniform over suitably long length in the remaining spatial dimension. The analysis of two-dimensional hierarchical structures is also of engineering relevance. Truss structures found in a wide range of applications are restrained such that the analysis is reduced to a two-dimensional optimization problem; roof and bridge truss structures serve as prime examples. Furthermore, many of the properties of the two-dimensional structure are likely to be found also in the three-dimensional counterpart (such as Refs. [10,14]), while the two-dimensional structures are more amenable to computational methods.

The structures considered in this article are typically referred to as imperfection insensitive [15]; this classification also applies to their three-dimensional counterparts such as those presented in Refs. [10,14]. These designs are often limited by excessive deflection [15]. It is found that in the case of the optimized structures considered here, the deflection of the imperfect structure on a global scale causes extra loading on the substructures and thus causes a local failure. While the structure is globally imperfection insensitive, local buckling gives a natural failure definition.

I. OPTIMIZATION OF THE PERFECT HIERARCHICAL FRAME

The hierarchical structure considered here is generated through an iterative process. The generation-0 structure is a simple solid beam: A simple truss structure made up of solid beams represents a generation-1 structure (see Fig. 1). The generation-2 structure is created by replacing all simple beams in the generation-1 structure with scaled generation-1 frames. Higher-order structures can be obtained through the same replacement procedure. The notation here will follow that used in related works [8,9]: $X_{G,i}$ represents the parameter X at the ith hierarchical level ($i = 0$ being the smallest and $i = G$ being the largest) of a structure with $G + 1$ characteristic length scales.

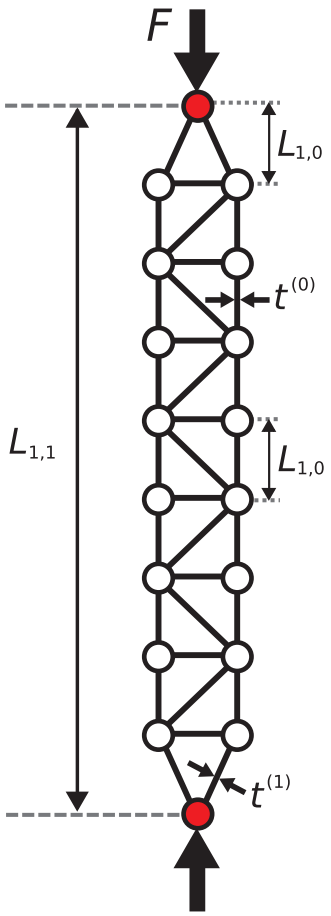

FIG. 1. (Color online) Generation-1 structure and notation used throughout this paper.

A. Generation 0

For the purposes of comparison, a freely hinged beam of length L made from an isotropic material, in two dimensions, will be termed a generation-0 structure. We introduce F as a loading parameter with dimension MT^{-2}. This can be thought of as force per unit length of structure in the remaining spatial dimension. Assuming plane strain conditions, this beam will fail when the applied load F on the beam reaches the Euler buckling load [16]

$$F = \frac{\pi^2 D}{L^2}, \tag{1}$$

where D is the flexural rigidity of the structure. A beam of thickness t in two dimensions can be seen to have a flexural rigidity of

$$D = \frac{Yt^3}{12(1-\nu^2)}, \tag{2}$$

where Y and ν are the Young's modulus and Poisson ratio of the material, respectively [17]. The frames we describe here are hierarchical or fractal over a finite range of length scales. In bulk materials with a hierarchical microstructure, it is sometimes useful to calculate effective scale-dependent elastic moduli [18]; however, in our calculations we do not do this: Y is the Young's modulus of the material itself, defined at the smallest continuum scale (much smaller than the smallest mechanical member of our structures and much larger than the atomic scale). It is not a scale-dependent parameter. We define the nondimensional variables

$$f \equiv \frac{F(1-\nu^2)}{YL}, \tag{3}$$

$$v \equiv \frac{V}{L^2}, \tag{4}$$

where V is the volume of the structure per unit length into the page (that is to say, its cross-sectional area). It is straightforward to show that in the case of a generation-0 structure, the scaling of nondimensional material v required to make a stable structure under the nondimensional load f is

$$v \sim f^{1/3}. \tag{5}$$

Here we investigate the limit of gentle loading, or $f \ll 1$, thus higher powers of f in the above expression lead to a decrease in the required volume to create a stable structure under a given loading f.

B. Generation 1

The generation-1 structure considered here is a simple frame with end points at (0,0) and ($L_{1,1}$,0) as shown in Fig. 1. If the length of each constituent vertical or horizontal beam is $L_{1,0}$, then it can be shown that this length is related to the length of the whole frame $L_{1,1}$ through the expression

$$L_{1,1} = (n_{1,1} + 2)L_{1,0}, \tag{6}$$

where $n_{1,1}$ is the number of box sections in the frame (in the example shown in Fig. 1, $n_{1,1} = 7$). If the loading on the entire frame is $F_{1,1}$, each of the vertical constituent beams of length $L_{1,0}$ supports the load

$$F_{1,0} = \frac{F_{1,1}}{2}. \tag{7}$$

We note that the generation-1 structure has two modes of failure: the first, the local failure of a constituent beam; the second, the global failure of the whole structure. For convenience we define

$$f_0 \equiv \frac{F_{G,0}(1-\nu^2)}{YL_{G,0}}. \tag{8}$$

Using Eqs. (1), (2), (7), and (8), it is found that the thickness of the constituent vertical beams such that they are on the point of failure by Euler buckling is given by

$$t^{(0)} = L_{1,0}\left(\frac{12 f_0}{\pi^2}\right)^{1/3}. \tag{9}$$

Due to the geometry of the frame, the end beams support an increased loading when compared to the vertical beams. They also span a greater length; thus an increased value of t is required for stability. The critical value of thickness for these beams is

$$t^{(1)} = L_{1,0}\left(\frac{15\sqrt{5}}{2}\frac{f_0}{\pi^2}\right)^{1/3}. \tag{10}$$

In the perfect truss structure, the diagonal beams within the box sections resist no loading but are necessary for rigidity of the frame. It is noted that by having a spring constant of diagonal and horizontal beams in the structure similar to that of the vertical beams, the generation-1 structure behaves as a Euler-Bernoulli beam under deformation; thus their thickness is set to $t^{(0)}$. The flexural rigidity of the composite frame is dominated by the contributions from the beams furthest from the neutral axis of the frame [17]. Thus it can be approximated by

$$D_{1,1} \approx \frac{Y t^{(0)} L_{1,0}^2}{2(1-\nu^2)}. \tag{11}$$

This approximation becomes more precise with increasing $n_{1,1}$. Using Eqs. (1) and (10), it can be shown that for the whole structure to be on the point of global failure

$$n_{1,1} = \left\lfloor -2 + \sqrt{\frac{\pi^{4/3} 12^{1/3}}{4 f_0^{2/3}}} \right\rfloor, \tag{12}$$

where $\lfloor \cdot \rfloor$ is the floor function. Then, using Eqs. (3) and (6)–(8), it is found that

$$f = \frac{4 f_0^{4/3}}{\pi^{2/3} 12^{1/6}}. \tag{13}$$

It is found that the volume of the generation-1 structure is given by

$$V(1) = [(3+\sqrt{2}) n_{1,1} + 6] L_{G,0} t^{(0)} \tag{14}$$

and using Eqs. (4), (9), (10), (12), and (14) we obtain

$$v \approx \frac{2(3+\sqrt{2}) 12^{1/6}}{\pi^{4/3}} f_0^{2/3} - \frac{8\sqrt{2}}{\pi^2} f_0. \tag{15}$$

Thus, we see to leading order

$$v \sim f^{1/2}, \tag{16}$$

showing greater efficiency in the limit of light loading when compared to the generation-0 structure.

C. Generation 2

To construct the generation-2 truss structure, all simple beams in the generation-1 design are replaced with scaled generation-1 frames. Part of a generation-2 structure is shown in Fig. 2, where the terminology for the generation-2 frame is also introduced. We observe that all the scaled generation-1 subframes that resist compression are under one of two loading conditions: either that experienced by the subframes connected directly to the end points or the reduced load and length of the subframes parallel to the neutral axis of the generation-2 structure. We define $L_{G,0}$ to be the length of the simple beams bearing compression in the central subframes (see Fig. 2). For the component beams in the vertical subframes to be on the point of failure, using Eqs. (1), (2), and (8), their component beam thicknesses must be given by

$$t^{(0)} = \left(\frac{12 f_0}{\pi^2}\right)^{1/3} L_{2,0}, \tag{17}$$

$$t^{(1)} = \left(\frac{15\sqrt{5}}{2} \frac{f_0}{\pi^2}\right)^{1/3} L_{2,0}, \tag{18}$$

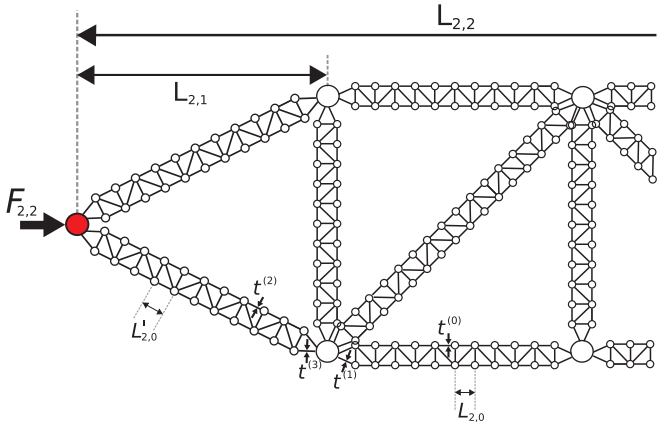

FIG. 2. (Color online) Section of the generation-2 frame and the parameters that describe it. Here the frame has been rotated through $\frac{\pi}{2}$ compared to Fig. 1.

where $t^{(0)}$ and $t^{(1)}$ are the thicknesses of the central and end beams respectively (as shown in Fig. 2). Then, through stating that the central subtrusses themselves must be on the point of failure, through use of Eqs. (1), (6), (11), and (17), $n_{2,1}$ is found to be

$$n_{2,1} = \left\lfloor -2 + \sqrt{\frac{\pi^{4/3} 12^{1/3}}{4 f_0^{2/3}}} \right\rfloor. \tag{19}$$

For the subframes connected directly to the loading points of the generation-2 frame two parameters are introduced: $L'_{2,0}$ is the length of the shortest beams that make up the subframe and $n'_{2,1}$ is the number of box sections that make up the subframe. Then, using Eqs. (1), (2), and (8) and specifying that all component beams are on the point of failure, it is found that

$$t^{(2)} = \left(\frac{6\sqrt{5} f_0}{\pi^2}\right)^{1/3} \left(L'^2_{2,0} L_{2,0}\right)^{1/3}, \tag{20}$$

$$t^{(3)} = \left(\frac{75}{4} \frac{f_0}{\pi^2}\right)^{1/3} \left(L'^2_{2,0} L_{2,0}\right)^{1/3}. \tag{21}$$

By stating that the end frames must also be on the point of failure and noting that $L_{2,1} = (n_{2,1}+2) L_{2,0} = \frac{2}{\sqrt{5}} (n'_{2,1}+2) L'_{2,0}$ it can be shown that

$$n'_{2,1} = n_{2,1}. \tag{22}$$

Therefore, Eqs. (20) and (21) become

$$t^{(2)} = t^{(1)}, \tag{23}$$

$$t^{(3)} = \left(\frac{375}{16} \frac{f_0}{\pi^2}\right)^{1/3} L_{2,0}. \tag{24}$$

We choose that the generation-1 subframes perpendicular to the long axis of the generation-2 structure take the same parameters as those parallel to the neutral axis. The diagonal, longer subframes differ from these structures only by a factor of $\sqrt{2}$ in the length of their component beams. In the perfect frame, these structures bear no compressive load.

Due to the geometry of the truss, we note that all the simple beams that resist compression have equal spring constants. This universal spring constant for all simple compression bearing beams is found to be

$$k_{2,0} = Y\left(\frac{12 f_0}{\pi^2}\right)^{1/3}. \tag{25}$$

The spring constants of the compression bearing generation-i frames (or subframes) are given by

$$k_{2,i} = \frac{8k_{2,i-1}}{4n + 5\sqrt{5} + 1}. \tag{26}$$

We note the spring constants of the generation-1 compression bearing subframes are independent of the load they resist. It can be shown, through direct calculation including only the contribution from those beams parallel to the neutral axis of the entire structure (neglecting the effects of the end triangles at both hierarchical levels), that the flexural rigidity of the generation-2 frame is approximated by

$$D_{2,2} \approx \frac{Y L_{2,1}^2 t^{(0)}}{1-\nu^2}. \tag{27}$$

Given that

$$L_{2,2} = (n_{2,2} + 2)L_{2,1}, \tag{28}$$

$$F_{2,2} = 2F_{2,1}, \tag{29}$$

it can be shown that for the whole generation-2 structure to be on the point of failure

$$n_{2,2} = n_{2,1}. \tag{30}$$

The total volume of the generation-2 truss structure can be shown to be

$$V(2) = [(3+\sqrt{2})n_{2,2} + 6]^2 L_{2,0} t^{(0)}. \tag{31}$$

Using Eqs. (3), (6)–(8), (28), and (29), it is found that

$$f = \frac{16}{\pi^{4/3} 12^{1/3}} f_0^{5/3}. \tag{32}$$

Thus, it can be shown that, to leading order,

$$v \sim f^{3/5}, \tag{33}$$

which shows a further gain in efficiency when compared to the generation-1 structure in the limit of light loading.

D. Generation G

The generation-G structure can be created using an iterative process. The generation-G frame is created by taking a generation-$(G-1)$ frame and replacing all simple beams scaled with generation-1 frames. The generation of the structure G is defined as the number of iterations of this procedure that have taken place. We see that, due to the geometry of the generation-1 design, for a given hierarchical level, the length of any subframe or beam will be dependent on the position within the frame. It can be shown that for the beams or subframes of minimal length at each hierarchical level

$$L_{G,i} = (n_{G,i} + 2)L_{G,i-1}, \tag{34}$$

$$D_{G,i} \approx \frac{2^{i-2} Y L_{G,i-1}^2 t^{(0)}}{1-\nu^2}, \tag{35}$$

$$F_{G,i} = 2F_{G,i-1}. \tag{36}$$

We note that $D_{G,i}$ has been calculated directly by considering the contributions of all beams parallel to the vertical axis of the generation-G frame; the effect of the end beams at each hierarchical level is not included. We note further that this approximation becomes more precise with increasing values of $n_{G,i}$. If we specify that

$$n_{G,i} = \left\lfloor -2 + \sqrt{\frac{\pi^{4/3} 12^{1/3}}{4 f_0^{2/3}}} \right\rfloor \quad \text{for} \quad 1 \leqslant i \leqslant G \tag{37}$$

for all frames and subframes regardless of i and position in the structure, then it is found that all subframes and simple beams under compressive load will have lengths within the set $\{L_{G,i}^{(n)}\}$, where

$$L_{G,i}^{(n)} = \left(\frac{\sqrt{5}}{2}\right)^n L_{G,i}, \quad 0 \leqslant n \leqslant G - i, \tag{38}$$

and $L_{G,i}$ is the minimum length of all subframes or beams at that particular hierarchical level. These subframes or beams of minimum length will be those passing through $x = \frac{L_{G,G}}{2}$ (assuming n is odd). From the geometry of the frame, it can be shown that each simple beam with length $L_{G,0}^{(n)}$ will take the loading of

$$F_{G,0}^{(n)} = \left(\frac{\sqrt{5}}{2}\right)^n F_{G,0}, \tag{39}$$

where n takes the same value as in Eq. (38) with $i = 0$. It can therefore be shown that for every beam under compressive loading to be on the point of failure

$$t^{(n)} = \left(\frac{\sqrt{5}}{2}\right)^n \left(\frac{12 f_0}{\pi^2}\right)^{1/3}. \tag{40}$$

The parameters $X_{G,i}$ describing subframes at level i perpendicular to the neutral of the frame (or subframe) at level $i+1$ are chosen to be identical those subframes parallel to the neutral axis. We choose that the diagonal subframes within each box section take the same values of beam thickness and n as the subframes that enclose them; the length of the component beams, however, is a factor of $\sqrt{2}$ greater than the equivalent beam in the surrounding subframes. In the perfect structure, these subframes experience no compressive load. In a frame containing small imperfections of the type described in this paper, they are significantly overengineered.

Considering the volume of a generation-G truss structure, we find that

$$V(G) = [(3+\sqrt{2})n + 6]^G L_{2,0} t^{(0)}. \tag{41}$$

Furthermore, it can be shown that, for all $G > 1$,

$$f = 2^{2G}\left(\frac{1}{\pi^{4/3} 12^{1/3}}\right)^{G/2} f_0^{1+G/3}. \tag{42}$$

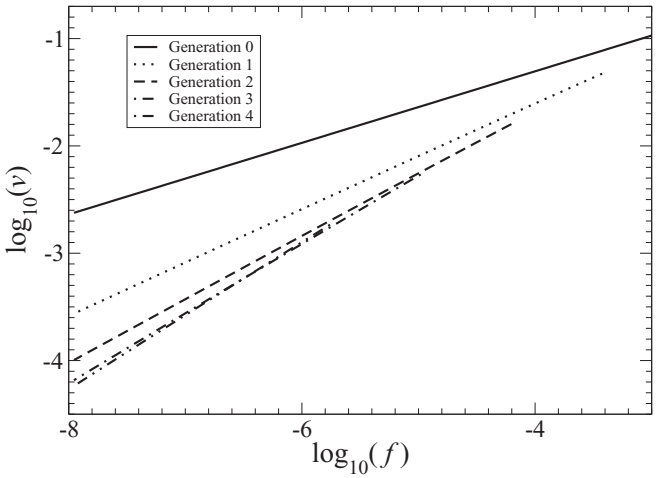

FIG. 3. Nondimensional volume against loading parameter for generation-0 to -4 designs shown on a log-log scale. Curves are only plotted when the structures involved are suitably slender for the approximation in Eq. (35) to be valid.

Then, through use of Eq. (4), (34)–(37), (40), and (41) we obtain, to leading order,

$$v \sim f^{(G+1)/(G+3)}, \tag{43}$$

which shows in the limit of small f that increasing the hierarchical order of the structure leads to an increase in efficiency. In Fig. 3 a log-log plot of v against f is shown for generations 0 to 4. The Hausdorff dimension of the optimal structure is also calculated and its dependence on loading is shown in Fig. 4.

II. IMPERFECTIONS IN THE HIERARCHICAL FRAME

Here we model the effect of an initial imperfection in a hierarchical frame. Through analytic models, we obtain the effect of a single beam's thickness being perturbed in a generation-1 and -2 frames. We find that for both strengthening and weakening the individual beam, the failure loading for the frame is reduced due to the introduction of asymmetry. Through finite-element methods, a generation-1 frame is analyzed with the same single-beam perturbation. Good agreement between finite-element and analytic models is found.

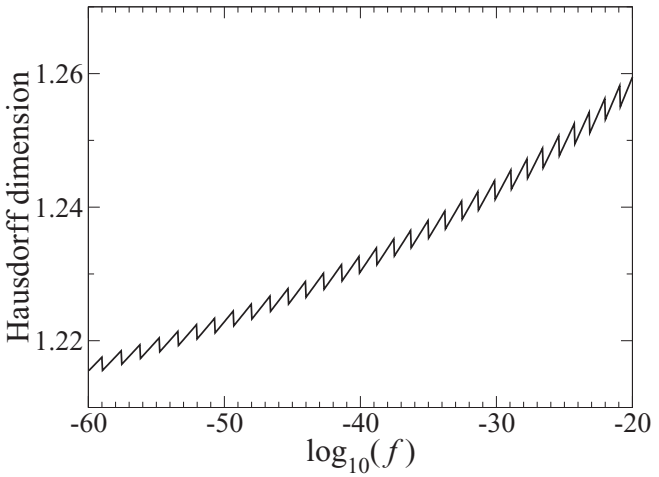

FIG. 4. Evolution of the fractal dimension of the optimal structure against the loading for which it is optimized. We note that this is not a function of applied load but a product of the optimization process. Discontinuities represent changes in optimal generation with increasing generations being favorable at smaller loading parameters.

A. Generation-1 analytic

We choose to model a simple imperfection: A single beam's thickness is perturbed from t to $t + \Delta t$. We take the perturbed beam to be a vertical beam halfway up the length of the frame with nodes at $(-\frac{L_{1,1}}{2}, \frac{L_{1,1}\pm L_{1,0}}{2})$ (assuming $n_{1,1}$ is odd).

1. Deformation under loading

In the limit of small loading, the perturbed beam will experience a load of $\frac{F_{1,1}}{2}$ and have a spring constant different from all other beams in the frame. Thus, as shown in Fig. 5, asymmetry will be introduced into the deformation of the frame. Globally, the deformation of the neutral axis of the truss $y^0_{1,1}$ can be expressed as

$$y^0_{1,1}(x) = \begin{cases} \frac{2a_{1,1}x}{L_{1,1}-L_{1,0}}, & x \in \left[0, \frac{(n+1)L_{1,0}}{2}\right] \\ a_{1,1}, & x \in \left[\frac{(n+1)L_{1,0}}{2}, \frac{(n+3)L_{1,0}}{2}\right] \\ 2a_{1,1} - \frac{2a_{1,1}x}{L_{1,1}+L_{1,0}}, & x \in \left[\frac{(n+3)L_{1,0}}{2}, L_{1,1}\right], \end{cases} \tag{44}$$

where $a_{1,1}$ is the magnitude of the deflection and is given by

$$a_{1,1} = \left(\frac{L_{1,1}-L_{1,0}}{2} - \frac{F_{1,1}}{k'_{1,1}}\right) \frac{F_{1,0}\Delta t}{2Yt^{(0)}(t^{(0)}+\Delta t)}. \tag{45}$$

Above, $k'_{1,1}$ is the spring constant of the frame above the perturbed beam (that is, of the triangle and $\frac{n_{1,1}-1}{2}$ box sections). The deformation of the entire frame [Eq. (44)] can be written as an infinite Fourier series [19]

$$y^0_{1,1} = \frac{8a_{1,1}}{\pi^2} \sum_{k=0}^{\infty} (-1)^k \frac{\sin\left[(2k+1)\frac{\pi x}{L_{1,1}}\right]}{(2k+1)^2}, \quad k \in \mathbb{Z}. \tag{46}$$

For larger compressive forces the deflection of the neutral axis will not remain as in Eq. (44). The total deflection of the frame will then be described as

$$y_{1,1} = y^0_{1,1} + y^1_{1,1}, \tag{47}$$

where $y^0_{1,1}$ is the dominant deflection for small loading and $y^1_{1,1}$ is the deformation caused by the further compression of the truss. The evolution of $y^1_{1,1}$ is governed by the differential equation

$$YI_{1,1}\frac{d^2y^1_{1,1}}{dx^2} = -F_{1,1}\left(y^0_{1,1} + y^1_{1,1}\right). \tag{48}$$

Following the analysis of Timoshenko and Gere [17], it can be shown that the total deformation of the frame is given by

$$\begin{aligned} y_{1,1} &= \left(1 + \frac{F_{1,1}}{F^c_{1,1}}\right) \frac{8a_{1,1}}{\pi^2} \left[\frac{1}{1-\frac{F_{1,1}}{F^c_{1,1}}} \sin\left(\frac{x\pi}{L_{1,1}}\right) - \cdots\right] \\ &= A_{1,1} \sin\left(\frac{\pi x}{L_{1,1}}\right) - \cdots. \end{aligned} \tag{49}$$

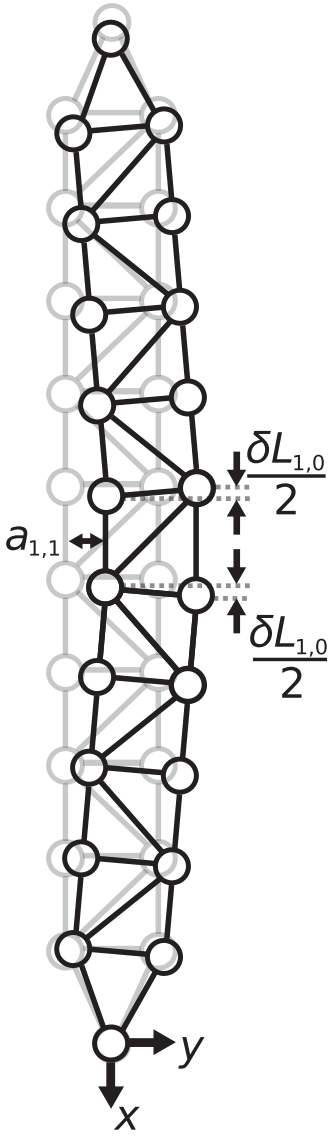

FIG. 5. Schematic showing the triangular deflection of a generation-1 frame caused by the weakening of the beam halfway up the frame on the left or by strengthening of the beam halfway up the frame on the right.

It is seen that in the region of $F_{1,1} \approx F^c_{1,1}$ the series in Eq. (49) is dominated by the first term in the expansion. The nature of the bifurcation of the perfect system with a critical point at the Euler buckling load is known as a stable-symmetric bifurcation [20]. This is where in the imperfect truss structure there is no point of failure analogous to the critical point of Euler buckling for the perfect frame. Instead, for the perturbed system, the deflection increases rapidly as the Euler load is approached.

2. *Effects of curvature*

We now investigate the effect of imposing a sinusoidal deflection on the neutral axis of a generation-1 frame. It is noted that as the loading approaches the Euler limit, the imperfect frame described above takes deflection of this form. Imposing a deformation from the initial straight configuration of

$$y = a \sin\left(\frac{\pi x}{L_{1,1}}\right) \tag{50}$$

will cause a curvature in the frame, which will result in a difference in length between the inner and outer beams in the frame $\delta L^C_{1,0}$. If $R_{1,1}$ represents the radius of curvature of the frame, it can be shown that

$$\Theta_{1,1} R_{1,1} = L_{1,0}, \tag{51}$$

$$\Theta_{1,1}\left(R_{1,1} - \frac{L_{1,0}}{2}\right) = L_{1,0} - \delta L^C_{1,0} \tag{52}$$

will be satisfied for some $\Theta_{1,1}$. In obtaining the above expressions we have made the assumption that the whole generation-1 frame behaves as a Euler-Bernoulli beam. The radius of curvature is related to lateral displacement of the frame by

$$\frac{1}{R_{1,1}} \approx \left|\frac{d^2 y}{dx^2}\right|. \tag{53}$$

It is observed that the radius of curvature will be minimal at $x = \frac{L}{2}$. The maximal value of $\delta L^C_{1,0}$ can therefore be related to a in Eq. (50) through the expression

$$\delta L^C_{1,0} = \frac{L^2_{1,0} a \pi^2}{2 L^2_{1,1}}. \tag{54}$$

Assuming Hookean behavior of the component beams, this increased compression signifies an increased loading on the beam.

3. *Failure criteria*

The critical point on the fundamental path of the generation-1 truss structure representing Euler buckling does not exist on the fundamental path of the imperfect structure. Instead, the deflection of the structure increases significantly as the Euler loading value is approached [11]. Due to the deflection of the structure, the loading on the component beams will be increased. Thus, we define failure of the whole structure to be when any component beam fails due to Euler buckling. The maximal loading on an individual beam in the generation-1 imperfect structure will be in the center of the truss, where the curvature is at its greatest. Here the beam on the inside of the curvature will experience a maximal loading $F^M_{1,0}$ of

$$F^M_{1,0} = F_{1,0} + k^{(0)}_{1,0} \delta L^C_{1,0}, \tag{55}$$

where $F_{1,0}$ is the loading on the vertical component beams in the perfect truss structure. Equating $F^M_{1,0}$ with the Euler buckling load of the component beams as given by Eqs. (1) and (2), we can find the value of $A_{1,1}$ that will lead to failure of the component beams. This is found to be

$$A^c_{1,1} = \frac{2L^2_{1,1}}{\pi^2 L^2_{1,0}}\left(\frac{\pi^2 (t^{(0)})^2}{12 L_{1,0}} - \frac{F_{1,0}}{k_{1,0}}\right). \tag{56}$$

Through equating the coefficient of $\sin(\frac{\pi x}{L})$ in Eq. (49) with Eq. (56), the loading at failure of the generation-1 beam with a single imperfection can be calculated. The evolution of $A_{1,1}$ predicted by Eq. (49) is plotted in Fig. 6 against loading for

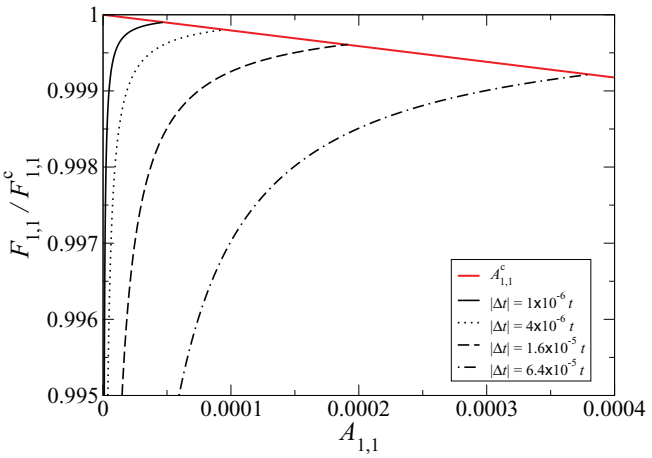

FIG. 6. (Color online) Evolution of $A_{1,1}$ as predicted by Eq. (49) along with its critical value from Eq. (56). The particular frame shown is optimized for $f = 7.59 \times 10^{-8}$ ($n_{1,1} = 101$).

various imperfection magnitudes; also shown is the figure is the critical value of $A_{1,1}$ given in Eq. (56).

The above analysis is only valid, however, in the case where the failure loading is very close to the Euler loading limit of the frame. If Δt is large enough and negative, failure occurs before the global deformation contributes significantly to the stress experienced by the perturbed beam. Failure in this case will simply follow the Euler load of the simple beam with a decreased width $t - |\Delta t|$. An important prediction of this analysis is that any asymmetric perturbation of a component beam, be it decreasing or increasing the thickness, will lead to a decrease in overall failure load of the composite structure.

Plotted in Fig. 7 is the value of the loading parameter at which a particular frame will fail against the magnitude of imperfection for both $\Delta t > 0$ and $\Delta t < 0$.

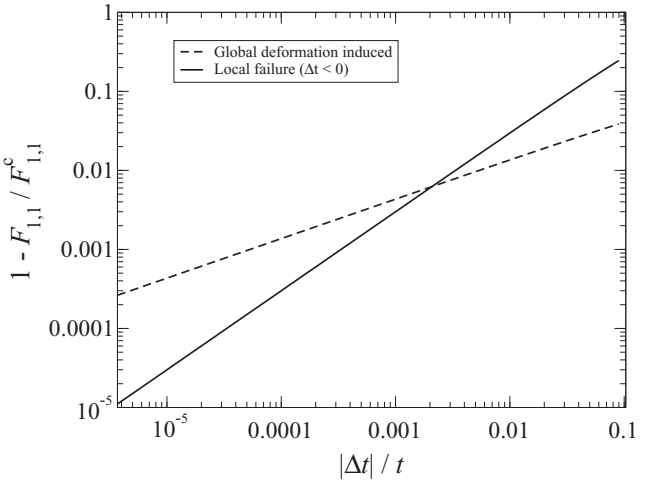

FIG. 7. Effect of a perturbation to one central beam for a particular frame optimized for $f = 1.08 \times 10^{-6}$ ($n = 51$). It is expected that for $\Delta t > 0$ the failure loading will always be induced by global deformation of the frame, whereas for $\Delta t < 0$, for small Δt global deflection will dominate while for larger Δt the local failure mode will dominate.

Defining

$$\Lambda \equiv 1 - \frac{F_{1,1}}{F^c_{1,1}}, \tag{57}$$

$$\xi \equiv \frac{\Delta t}{t}, \tag{58}$$

it can be seen that for optimized frame, independent of loading for which the frame is optimized, for small ξ,

$$\Lambda = \kappa_{1,1}\, \xi^{\alpha}, \tag{59}$$

where the value of $\alpha = 0.5 \pm 0.02$.

B. Generation 2

Here the effect of perturbing a single central beam in a generation-2 frame is established. We again choose the perturbed beam to be placed halfway up the generation-2 frame with nodes at $(-\frac{L_{2,1}+L_{2,0}}{2}, \frac{L_{2,2}\pm L_{2,0}}{2})$ (assuming n is odd).

1. Deformation under loading

Under light loading, the generation-1 subframe that contains the imperfection will deform from its initial straight configuration into a triangular wave whose deflection is given by

$$y^0_{2,1}(x') = \begin{cases} \frac{2a_{2,1}x'}{L_{2,1}-L_{2,0}}, & x' \in \left[0, \frac{(n+1)L_{2,0}}{2}\right] \\ a_{2,1}, & x' \in \left[\frac{(n+1)L_{2,0}}{2}, \frac{(n+3)L_{2,0}}{2}\right] \\ 2a_{2,1} - \frac{2a_{2,1}x'}{L_{2,1}+L_{2,0}}, & x' \in \left[\frac{(n+3)L_{2,0}}{2}, L_{2,1}\right], \end{cases} \tag{60}$$

where x' is related to the global coordinate system by $x' = x + \frac{L_{2,1}+L_{2,0}}{2}$ and $y^0_{2,1}$ represents the lateral displacement of the imperfect generation-1 frame relative to the initial, straight, configuration. This is shown in the inset of Fig. 8. The value of $a_{2,1}$ can be shown to be

$$a_{2,1} = \left(\frac{L_{2,1} - L_{2,0}}{2} - \frac{F_{2,1}}{k'_{2,1}}\right) \frac{F_{2,0}\Delta t}{2Yt^{(0)}(t^{(0)} + \Delta t)}. \tag{61}$$

It is straightforward to see that a displacement of the form of Eq. (60) will cause a difference in the end-to-end length of the imperfect frame and its perfect counterpart. This difference is found to be

$$\delta L_{2,1} = (n+1)L_{2,0} - 2\sqrt{\left(\frac{n+1}{2}L_{2,0}\right)^2 - a^2_{2,1}} + \frac{F_{2,0}}{k^{(0)}_{2,0}}\left(1 - \frac{2t^{(0)} + \Delta t}{k^{(0)}_{2,0}(t^{(0)} + \Delta t)}\right). \tag{62}$$

The first two terms in Eq. (62) are due to the lateral displacement of the imperfect frame, while the latter term is due to the central square unit cell deforming into a trapezium under loading. As shown in Fig. 8, a difference in end-to-end length in the central generation-1 subframes will lead to a global deflection in the generation-2 frame. For small values

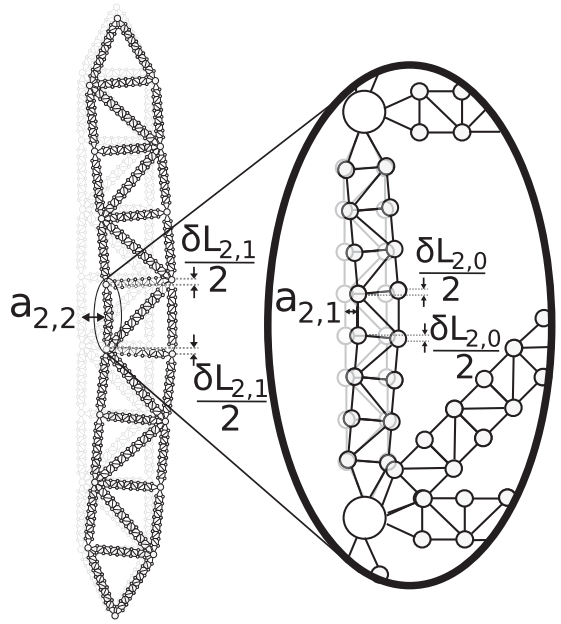

FIG. 8. Deformation for the early stages of loading for the generation-2 frame. The perturbed beam is the simple beam halfway up the enlarged generation-1 subframe on the left-hand side (assuming $\Delta t < 0$).

of compressive load, the deflection will take the form

$$y^0_{2,2}(x) = \begin{cases} \frac{2a_{2,2}x}{L_{2,2}-L_{2,1}}, & x \in \left[0, \frac{(n+1)L_{2,1}}{2}\right] \\ a_{2,2}, & x \in \left[\frac{(n+1)L_{2,1}}{2}, \frac{(n+3)L_{2,1}}{2}\right] \\ 2a_{2,2} - \frac{2a_{2,2}x}{L_{2,2}+L_{2,1}}, & x \in \left[\frac{(n+3)L_{2,1}}{2}, L_{2,2}\right], \end{cases} \tag{63}$$

where

$$a_{2,2} = \left(\frac{L_{2,2}-L_{2,1}}{2} - \frac{F_{2,2}}{k'_{2,2}}\right)\frac{\delta L_{2,1}}{2L_{2,1}}. \tag{64}$$

As in the case of generation-1 imperfect beam this can be written as a series

$$y^0_{2,2} = \frac{8a_{2,2}}{\pi^2}\sum_{k=0}^{\infty}(-1)^k \frac{\sin\left[(2k+1)\frac{\pi x}{L_{2,2}}\right]}{(2k+1)^2}, \quad k \in \mathbb{Z}. \tag{65}$$

When the frame is loaded further the deflection will deviate from the form given in Eq. (63); the evolution of this increased displacement $y^1_{2,2}$ will be governed by

$$YI_{2,2}\frac{d^2y^1_{2,2}}{dx^2} = -F_{2,2}\left(y^0_{2,2} + y^1_{2,2}\right). \tag{66}$$

As with the generation-1 frame, an expression showing the dependence of the displacement of the frame on the loading parameter can be obtained; a series solution analogous to Eq. (49) is found:

$$y_{2,2} = \left(1 + \frac{F_{2,2}}{F^c_{2,2}}\right)\frac{8a_{2,2}}{\pi^2}\left[\frac{1}{1-\frac{F_{2,2}}{F_{2,2}c}}\sin\left(\frac{\pi x}{L_{2,2}}\right) - \cdots\right]$$
$$= A_{2,2}\sin\left(\frac{\pi x}{L_{2,2}}\right) - \cdots. \tag{67}$$

In the vicinity of $F_{2,2} \approx F^c_{2,2}$ this expansion will be dominated by the first term. It is noted that in this loading regime, the generation-1 imperfect subframe will be deformed from its initial straight configuration by

$$y_{2,1} = \left(1 + \frac{F_{2,1}}{F^c_{2,1}}\right)\frac{8a_{2,1}}{\pi^2}\left[\frac{1}{1-\frac{F_{2,1}}{F^c_{2,1}}}\sin\left(\frac{x'\pi}{L_{2,1}}\right) - \cdots\right]$$
$$= A_{2,1}\sin\left(\frac{\pi x'}{L_{2,1}}\right) - \cdots. \tag{68}$$

2. Effects of curvature

Here we investigate the effect of imposing a sinusoidal deflection on the generation-2 structure. Under large loading, the imperfect truss structure will take deformation of this form. If the deflection is given by

$$y = a\sin\left(\frac{\pi x}{L_{2,2}}\right), \tag{69}$$

the truss will have a curvature induced. Using the approximation in Eq. (53), it is straightforward to show that the minimal radius of curvature of the global deformation $R_{2,2}$ is related to a in Eq. (69) by

$$\frac{1}{R_{2,2}} = \frac{\pi^2 a}{L^2_{2,2}}. \tag{70}$$

The curvature in the truss will cause a difference in end-to-end length in the generation-1 subtrusses at the center of the frame. Denoting the difference in end-to-end length of the central generation-1 subframes due to the curvature of the generation-2 frame by $\delta L^C_{2,1}$ and assuming that the whole generation-2 frame behaves as an Euler-Bernoulli beam, it can be shown that

$$\Theta_{2,2}R_{2,2} = L_{2,1}, \tag{71}$$

$$\Theta_{2,2}\left(R_{2,2} - \frac{L_{2,1}}{2}\right) = L_{2,1} - \delta L^C_{2,1} \tag{72}$$

will be satisfied for some value of $\Theta_{2,2}$. Combining Eqs. (70)–(72) it is seen that

$$\delta L^C_{2,1} = \frac{\pi^2 L^2_{2,1}a}{2L^2_{2,2}}. \tag{73}$$

3. Failure criteria

Due to the asymmetric imperfection in the truss structure, there will be no critical point of Euler buckling in the imperfect generation-2 frame or the imperfect generation-1 subframe. Instead, in both, the deflection $y_{G,i}$ will increase as the critical point of the perfect structure is approached. In this loading regime, the deflection of the imperfect generation-1 subframe and generation-2 frame will be given by Eqs. (44) and (63), respectively. As shown in Secs. II A 2 and II B 2, a deflection of this form causes an increase in loading of the beams and subframes on the inside of the curvature. The maximal value of loading for a generation-1 frame in the imperfect generation-2 structure can be calculated as

$$F^M_{2,1} = F_{2,1} + k^{(0)}_{2,1}\delta L^C_{2,1}, \tag{74}$$

where $F_{2,1}$ is the force experienced by a vertical subframe in the perfect structure and $\delta L^C_{2,1}$ is given by Eq. (73) with $a = A_{2,2}$. Through equating $F^M_{2,1}$ with the Euler buckling load of the generation-1 subtruss, as given by Eqs. (1) and (11), we can calculate the value of $A_{2,2}$ that will cause failure of a generation-1 subframe; this is found to be

$$A^c_{2,2} = \frac{2L^2_{2,2}}{\pi^2 L^2_{2,1}} \left(\frac{\pi^2 Y t^{(0)} L^2_{2,0}}{2k^{(0)}_{2,1} L^2_{2,1}} - \frac{F_{2,1}}{k^{(0)}_{2,1}} \right). \tag{75}$$

The maximal loading possible on a vertical component beam in the structure can then be calculated as

$$F^M_{2,0} = \frac{F^M_{2,1}}{2} + k^{(0)}_{2,0} \delta L^C_{2,0}, \tag{76}$$

where $\delta L^C_{2,0}$ is given by Eq. (54) with $a = A_{2,1}$. Again we can calculate the maximal value of $A_{2,1}$ permissible before the component beams fail as

$$A^c_{2,1} = \frac{2L^2_{2,1}}{\pi^2 L^2_{2,0}} \left(\frac{\pi^2 (t^{(0)})^2}{12 L_{2,0}} - \frac{F_{2,0}}{k_{2,0}} \right). \tag{77}$$

Then, through equating $A_{2,1}$ as predicted in Eq. (68) by replacing $F_{2,1} = F^M_{2,1}$ with $A^c_{2,1}$ and equating $A_{2,2}$ as predicted in Eq. (67) with $A^c_{2,2}$, we obtain the possible values of loading that lead to failure of the generation-2 imperfect truss structure. The values of loading that lead to these failures are shown in Fig. 9. It is found that for the generation-2 truss structure an imperfection, either strengthening or weakening a single component beam, causes a reduction in failure load for the whole structure. From Fig. 9 we see that the failure of the individual component beams occurs before the subframe failure for all values of loading. We see, however, that for large negative values of imperfections local buckling of the component beams occurs before significant deformation of the form (67) occurs. Using Eqs. (57) and (58), we find that for small perturbations

$$\Lambda = \kappa_{2,2} \xi^{\alpha}, \tag{78}$$

where $\alpha = 0.5 \pm 0.05$.

C. Simulations

It is noted that the expression relating the flexural rigidity of the truss structure and the frame parameters in Eq. (11) is not exact. This causes the local and global failure modes to be noncoincident in the loading procedure, leading to deviations from the behavior described above. In this section, results of finite-element simulations are shown against the theoretical predictions. The simulations are undertaken using the spherical arclength method (see Refs. [21,22]). Without exception, freely hinged joints are assumed at the nodes within the structure. Only generation-1 structures are investigated through simulation due to increased computational requirements for higher generations.

Equation (11) becomes more accurate in the limit of large $n_{1,1}$. When $n_{1,1}$ is relatively small, it is found that this formula overestimates the stability against global buckling when compared to the results of finite-element simulation. The value of $A^c_{1,1}$, as given in Eq. (56), is independent of $F^c_{1,1}$ and thus $A^c_{1,1}$ is not altered by any inaccuracy in Eq. (11). However, the evolution of $A_{1,1}$ as predicted in Eq. (49) is changed considerably by this inaccuracy. This is summarized in Fig. 10, where the evolution of $A_{1,1}$ found through simulation is shown for a frame optimized such that $n_{1,1} = 51$. The critical point found by simulation is 0.59% less than that predicted by Eq. (11). The evolution of $A_{1,1}$ can, however, still be predicted by Eq. (49) through substitution of the critical value of the

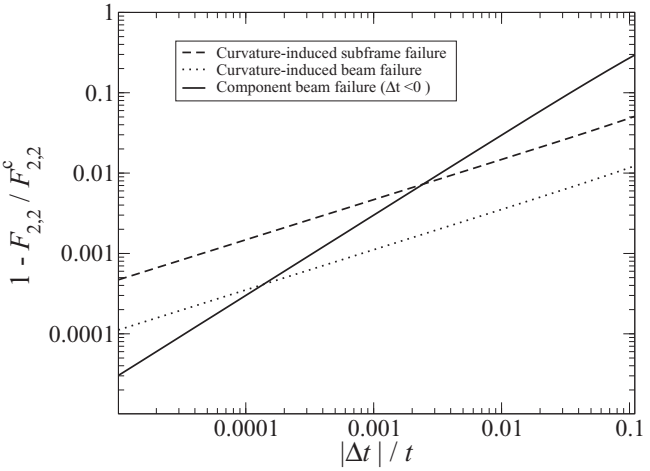

FIG. 9. Loading at failure for a particular imperfect generation-2 frame ($n_{2,2} = n_{2,1} = 101$) against magnitude of imperfection. Shown is a simple failure of the weakened beam ($\Delta t < 0$), the point at which $A^c_{2,1}$ is reached (labeled generation-0 bowing-induced failure), and the point of loading at which $A^c_{2,2}$ is reached (labeled generation-1 subframe failure). This particular plot is shown for $\Delta t < 0$; for $\Delta t > 0$ the functional dependence remains the same, however the generation-0 bowing-induced failure is translated a small amount towards increased stability.

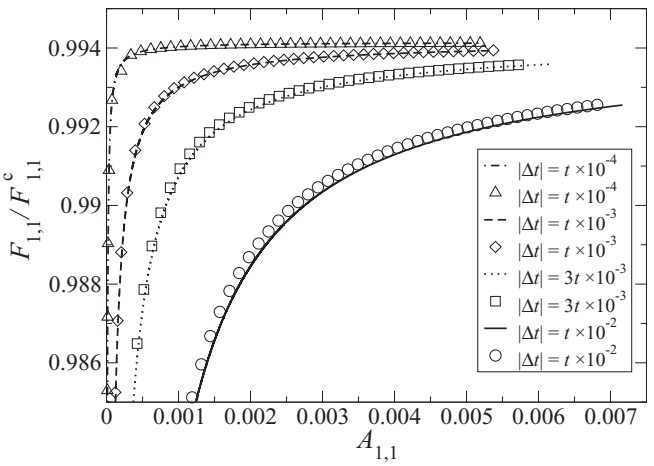

FIG. 10. Agreement between analytic prediction and simulation results for the evolution of the deformation in a frame with $n = 51$. Here $F^c_{1,1}$ refers to that found through use of Eq. (11); the critical point of the generation-1 frame is seen to be predicted to be greater through use of this equation compared to finite-element simulations. Plotted with lines are the analytic predictions for the evolution of the coefficient of the first term in Eq. (49) with increasing load, with symbols the results of simulation for the displacement of the central point of the frame in the x direction.

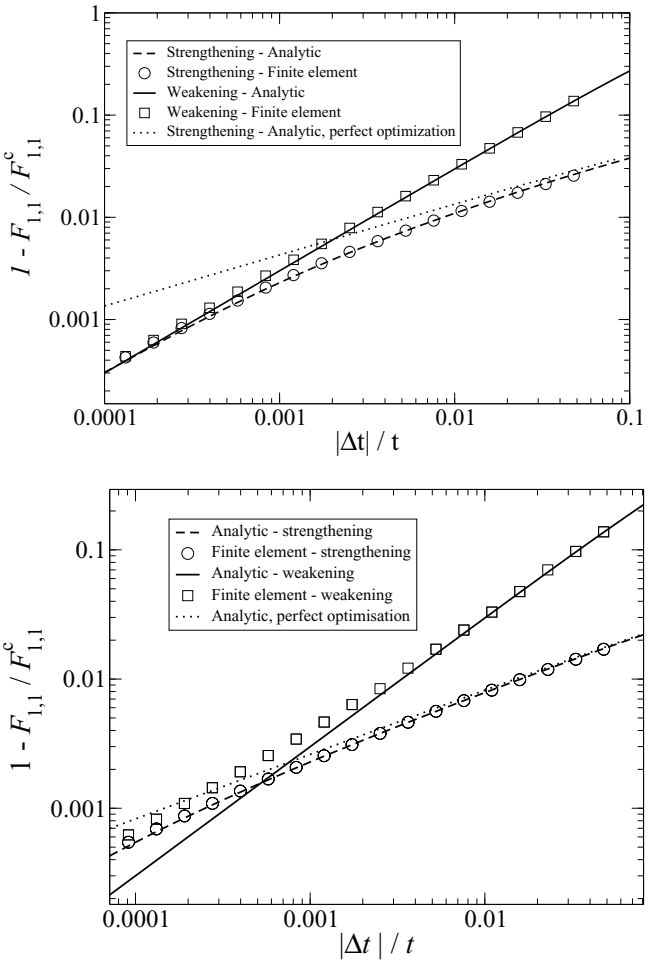

FIG. 11. Agreement between analytic predictions for the change in failure loading against the results of finite-element simulations. Also shown is the analytic result assuming Eq. (11) is exact. The top plot shows the results for $n_{1,1} = 51$ and the bottom the results for $n_{1,1} = 143$; for greater values of $n_{1,1}$ it is seen the half power law has an increased range of validity.

frame found through simulation in place of $F^c_{1,1}$ in Eq. (49); this is shown in Fig. 10, for various values of imperfection magnitude.

The power law relating imperfection to reduction in failure load can be tested through simulation. As above, the inaccuracy in Eq. (11) must be taken into account. Through substitution of the critical point found through simulation in place of $F^c_{1,1}$ in Eq. (49) and subsequently equating the coefficient of the first term with Eq. (56), the failure load of a given frame with a given imperfection can be predicted; this can then be tested against simulation. The results of both the corrected theory and simulation are shown in the top plot of Fig. 11 alongside those predictions that are valid for the perfect optimization for a frame optimized for loading of $f = 2.87 \times 10^{-5}$ ($n_{1,1} = 51$). Good agreement between theory and simulation for both signs of Δt is observed. The bottom plot of Fig. 11 shows the predictions made by analytic work and the results of finite-element simulations for a frame optimized such that $n_{1,1} = 143$ ($f = 2.04 \times 10^{-8}$); in particular one can see that, as a result of the increasing accuracy of Eq. (11), the half power law has an increased range of validity.

III. DISCUSSION

It has been shown that the principle of hierarchical design can be applied to a structure in two dimensions. As in three dimensions, increasing the hierarchical order of the structure can be seen to result in higher efficiency in the limit of low loading. The effect of a perturbation to a single central beam in the structure has been obtained theoretically for generations 1 and 2. It was found that the behavior of the generation-1 subframe dominates the effect of the imperfection in the generation-2 frame. This behavior is expected to apply to three-dimensional frames that display imperfection-insensitive behavior at the critical point of loading. In both generations 1 and 2 of the two-dimensional frame, a half power law relating imperfection magnitude to reduction in loading at failure was found. It was found that any asymmetric perturbation in the frame, be it strengthening or weakening the perturbed beam, results in a reduction in loading at failure. The results of analytic work in the case of generation-1 frames were confirmed through finite-element work. The effect of inaccuracies in the optimization procedure has also been discussed. Higher-generation frames are likely to exhibit the same behavior as discussed here. The one-half power law relating imperfection magnitude with reduction in failure load is expected to hold for general G. Modal interactions and distributions of imperfections remain as open topics for future work.

[1] H. Yao and H. Gao, J. Mech. Phys. Solids, **54**, 1120 (2006).
[2] J. Currey, *The Mechanical Adaptations of Bones* (Princeton University Press, Princeton, 1984).
[3] N. M. Hancox, *Biology of Bone* (Cambridge University Press, Cambridge, 1972).
[4] K. J. Koski, P. Akhenblit, K. McKiernan, and J. L. Yarger, Nat. Mater. **12**, 262 (2013).
[5] F. Bosia, M. J. Buehler, and N. M. Pugno, Phys. Rev. E **82**, 056103 (2010).
[6] R. S. Farr, Phys. Rev. E **76**, 056608 (2007).
[7] R. S. Farr, Phys. Rev. E **76**, 046601 (2007).
[8] D. Rayneau-Kirkhope, R. S. Farr, and Y. Mao, Europhys. Lett. **93**, 34002 (2011).
[9] D. Rayneau-Kirkhope, Y. Mao, and R. Farr, Phys. Rev. Lett. **109**, 204301 (2012).
[10] R. S. Farr and Y. Mao, Europhys. Lett. **84**, 14001 (2008).
[11] M. Ohsaki and K. Ikeda, *Stability and Opimistaion of Structures* (Springer, Berlin, 2007).
[12] *Structural Design Optimisation Considering Uncertainties*, edited by Y. Tsompanakis, N. D. Lagaros, and M. Papadrakakis (Taylor & Francis, London, 2008).
[13] K. Ikeda, K. Murota, and I. Ilishakoff, Comput. Struct. **59**, 463 (1996).

[14] D. Rayneau-Kirkhope, Y. Mao, R. Farr, and J. Segal, Mech. Res. Commun. **46**, 41 (2012).
[15] J. Roorda, *Buckling of Elastic Structures* (University of Waterloo Press, Waterloo, 1980).
[16] L. Euler, Mem. Acad. Sci. Berlin **13**, 252 (1759). Reprinted in: V. N. Vagliente and H. Krawinkler, J. Eng. Mech.-ASCE **113**, 186 (1987).
[17] S. P. Timoshenko and J. M. Gere, *Theory of Elastic Stability* (McGraw-Hill, New York, 1986).
[18] A. V. Dyksin, Int. J. Solids Struct. **42**, 477 (2005).
[19] K. F. Riley, M. P. Hobson, and S. J. Bence, *Mathematical Methods of Physics and Engineering* (Cambridge Univeristy Press, Cambridge, 1998).
[20] K. Ikeda and K. Murota, *Imperfect Bifurcation in Structures and Materials: Engineering Use of Group-Theoretic Bifurcation Theory* (Springer, Berlin, 2002).
[21] E. Riks, Int. J. Solids Struct. **15**, 529 (1979).
[22] M. A. Crisfield, Comput. Struct. **13**, 55 (1981).